atmosphere

Article

CHIMBO Air Quality Modeling System: Verification and Processes Analysis

Tony Christian Landi [1,*], Marco Paglione [1,*], Mauro Morichetti [2], Fabio Massimo Grasso [3], Fabrizio Roccato [1], Rita Cesari [3] and Oxana Drofa [1]

[1] National Research Council of Italy-Institute of Atmospheric Sciences and Climate (CNR-ISAC), 40129 Bologna, Italy
[2] National Research Council of Italy-Institute for Mediterranean Agricultural and Forestry Systems (CNR-Isafom), 06128 Perugia, Italy
[3] National Research Council of Italy-Institute of Atmospheric Sciences and Climate (CNR-ISAC), 73100 Lecce, Italy
* Correspondence: t.landi@isac.cnr.it (T.C.L.); m.paglione@isac.cnr.it (M.P.)

Abstract: This study presents an evaluation of the CHIMBO modeling chain applied to the Italian domain, specifically focusing on the Po Valley subdomain over the one-year period of 2019. The comparison between simulated and observed data indicates that the performance of the CHIMBO model aligns well with existing literature on other state-of-the-art models. The results demonstrate that the CHIMBO chain is particularly effective for regional-scale quantitative assessments of pollutant distribution, comparable to that of CAMS ensemble models. The analysis of key chemical species in particulate matter reveals that the CHIMBO model accurately represents the average concentrations of organic and elemental carbon, as well as secondary inorganic compounds (sulfate, nitrate, and ammonium), particularly at background monitoring stations in the flat terrain of the Po Valley, with the exception of Aosta, a city located at about 500 m asl. However, seasonal discrepancies were identified, especially during winter months, when significant underestimations were observed for several species, including elemental and organic carbon, predominantly at background sites. These underestimations are likely attributed to various factors: (i) inadequate estimations of primary emissions, particularly from domestic heating; (ii) the limited effectiveness of secondary formation processes under winter conditions characterized by low photochemical activity and high humidity; and (iii) excessive dilution of pollutants during calm wind conditions due to overestimation of wind intensity. In conclusion, while the CHIMBO modeling chain serves as a robust tool for mesoscale atmospheric composition investigations, limitations persist related to emissions inventories and meteorological parameters, which remain critical drivers of atmospheric processes.

Keywords: chemical transport model; mesoscale air quality modeling; Italy; Po Valley; PM chemical composition

Citation: Landi, T.C.; Paglione, M.; Morichetti, M.; Grasso, F.M.; Roccato, F.; Cesari, R.; Drofa, O. CHIMBO Air Quality Modeling System: Verification and Processes Analysis. *Atmosphere* **2024**, *15*, 1386. https://doi.org/10.3390/atmos15111386

Received: 17 October 2024
Revised: 12 November 2024
Accepted: 14 November 2024
Published: 17 November 2024

1. Introduction

Air pollution and understanding the processes that influence it are among the most important challenges facing most countries. The problem of air pollution requires action at the local, national and regional levels, as most sources of outdoor pollutants are beyond the control of individuals. Polluted air is present when the concentration of defined gases and particles, of both natural and anthropogenic origin, exceeds a certain concentration, with consequent adverse impacts on health, climate, cultural heritage, ecosystems and the economy [1]. The relationship between air quality and production processes was exacerbated by the Industrial Revolution in the late 1770s and early 20th century [2,3]. The interaction between air quality and health has been known since the London Smog phenomenon, dating back to 1852, which had very serious consequences for human health:

it is estimated that at least 4000 people died as a result of the fog, and many people subsequently suffered respiratory problems. There is currently very strong evidence of the negative impact of pollution on health, even with low concentrations of pollutants, as is evidenced by the World Health Organization (WHO) guidelines [4]. However, despite this awareness and pollution legislation, policies and investments supporting cleaner and modern [5,6] air pollution are among the greatest environmental risks to health. The WHO reported that in 2019, 99% of the world's population was living in places where air quality guidelines were not respected. Pollution-related death remains the second highest risk factor for noncommunicable diseases, and the combined effects of ambient (outdoor) air pollution and—for instance—household air pollution caused 6.7 million premature deaths in 2019, 4.2 million of which were due to outdoor air quality. This generally occurs in both urban and rural areas [4]. The adverse health effects are mainly due to exposure to ozone and fine particulate matter, which causes cancer and cardiovascular and respiratory diseases, such as ischemic heart disease, stroke and acute respiratory infections. Polluted air also has important effects on climate, as sources of pollutants are at the same time also sources of climate-altering substances. It is estimated that human activities caused a global warming of about 1 degree C in 2011–2020 above that in 1850–1900. The IPCC, through studied scenarios, finds that there is a more than 50% chance that global temperature rise will reach or exceed 1.5 degrees C in the near-term, even for the very low greenhouse gas emissions [7]. Besides, recent studies have related high pollutant concentrations and climate change to physical and aesthetic decay of cultural heritage [8–10]. Improving air quality thus brings benefits in terms of human health and environment but also in economic terms [11] Since the 1980s, the EU has adopted policies on air quality, setting air quality standards. Despite an overall improvement in air quality, the last European Environmental Agency (EEA) Report on Air Quality in Europe [12] states that in 2022, most of the EU's urban population continued to be exposed to levels of key air pollutants that are dangerous to health. With the ultimate goal of reducing the impact of air pollution on human health to a negligible level by 2050, the commission proposed in 2022 to revise the Air Quality Directives by introducing more ambitious air quality standards aligned with the recommendations of the World Health Organization [4]. The proposal is for the new standards to come into effect in 2030. In general, the directives set standards and measures to be carried out to reduce emissions and define common methods for air quality monitoring and assessment. The Directive 2008/50/EC 2008 states that "where possible modelling techniques should be applied to enable point data to be interpreted in terms of geographical distribution of concentration. This could serve as a basis for calculating the collective exposure of the population living in the area." The so-called chemistry and transport models take into account the relationships between meteorology, emissions, chemical reactions, deposition and pollutant concentrations [13,14]. The latest generation of models are able to include different types of sources, including natural emissions, such as biogenic emissions, mineral dust, vegetation fire and sea salt. In addition, models are being developed that take into account the interactions and feedback between different spatial scales and processes ([15–17] among many others). Numerical simulation of air quality enables scenario analysis, study of chemical and physical processes in the atmosphere, atmospheric composition analysis and forecast [18]. Currently, in Europe, in the framework of the Copernicus Atmosphere Monitoring Service (CAMS) [19], a forecasting system has been implemented that produces specific real-time air quality forecasts for the European domain at significantly higher spatial resolution (0.1 degrees, approx. 10 km) [20]. The production is based on an ensemble of eleven air quality forecasting systems across Europe (https://atmosphere.copernicus.eu/cams-european-air-quality-ensemble-forecasts-welcomes-two-new-state-art-models (accessed on 25 September 2024)). At the national scale, the CAMS National Collaboration Program Italy project has been active since 2022, which aims to consolidate and improve the performance of existing national models based on the Copernicus operational services. The Italian teams—mainly Consiglio Nazionale delle Ricerche (CNR), Ente Nazionale Energia ed Ambiente (ENEA) and Agenzia regionale per la prevenzione ambiente ed energie Emilia Romagna (ARPAE)—led by ISPRA (Istituto Superiore per la Protezione e la Ricerca ambientale, https://www.isprambiente.gov.it (accessed on 25 September 2024)), are modifying the national-scale air quality models to ingest the operational forecasts coming from the European-scale regional model "CAMS Regional Ensemble." The ultimate goal of the project is to detect and manage situations of high pollutant concentrations using CAMS data. In this project, the CNR-ISAC is currently participating using the CHIMBO modeling system. Further details on such international initiatives are available at the official National Collaboration Program web site (https://atmosphere.copernicus.eu/cams-national-collaboration-programme (accessed on 25 September 2024)).

This paper presents the first performance evaluation of the air quality forecast system CHIMBO, which is based on the BOLAM meteorological model [21] and the CHIMERE chemical transport model [22]. Currently, this is a unique air quality offline modeling system based on the meteorological model BOLAM developed at CNR-ISAC. The BOLAM model so far has been used only as meteorological driver in an online coupled meteorology-chemistry transport model (i.e., BOLCHEM [23]).

This work presents the first evaluation of the CHIMBO model covering the whole Italian national domain for a one-year period, providing key information about its skills and likely future applications. In particular, this paper shows the model performance to simulate the concentration of the main atmospheric pollutants, namely NO_2, O_3, PM_{10} and $PM_{2.5}$, at a national level (Italy) for the year 2019. Modeling results are compared with the CAMS ensemble model—used as a benchmark—together with the observations made available by the European Environmental Agency (EEA, https://discomap.eea.europa.eu/map/fme/AirQualityExport.htm (accessed on 25 September 2024)). Model verification for predicting the chemical composition of PM_{10} and/or $PM_{2.5}$ was performed over Northern Italy. In this area, from the Western Alps to the Adriatic Sea, the Po Valley is situated, which one of the most polluted areas in Europe [12,24]. The valley is highly populated, and several emission sources are present, such as industrial and agricultural activities, road transportation and livestock farming. The area is often affected by episodes of air stagnation, which promotes low pollutant dispersion and fog events in winter. These events impact the concentration level and toxicity of particulate matter [25–27]. Simulating air quality in the Po Valley is therefore a difficult task due to the above meteorological conditions of low-wind, and it is therefore of particular interest to test the performance of the model in such a complex area [28–32].

2. Materials and Methods

2.1. CHIMBO Modeling Chain: Model Description and Set up

CHIMBO is an air quality modeling system based on the Chemical Transport Model CHIMERE (https://www.lmd.polytechnique.fr/chimere (accessed on 25 September 2024)) and the meteorological model BOLAM (https://www.isac.cnr.it/dinamica/projects/forecasts/ (accessed on 25 September 2024)), coupled in offline mode. Figure 1 depicts the integration domains on which CHIMBO had run daily since August 2018, generating air quality forecasts up to 3 days ahead. Forecasts are freely available at the CHIMBO official web site: https://www.isac.cnr.it/dinamica/projects/forecasts/chimbo (accessed on 25 September 2024).

The meteorological model BOLAM [21] is a limited-area hydrostatic model that integrates the primitive equations using parametrization for the atmospheric convection. The horizontal discretization is based on a staggered Arakawa-C grid in geographical coordinates (latitude-longitude). In the vertical discretization, the prognostic variables are distributed on a non-regular Lorenz grid, with higher resolution near the lower surface of the atmospheric boundary layer. BOLAM was developed at CNR-ISAC of Bologna and has been extensively validated in numerous case studies and model intercomparison experiments [33–35]. It has also been used in operational weather forecasting, e.g., at the Centro Funzionale MeteoIdrologico di Protezione Civile of Liguria Region (ARPAL

CFMI-PC), at the National Observatory of Athens [35], at Servizio Agrometeorologico Regionale—Sardegna. In recent years, BOLAM has been used as the meteorological component of the online model BOLCHEM [23], in which it is integrated online with the gas chemistry module SAPRC90 and the aerosol dynamic module AERO3.

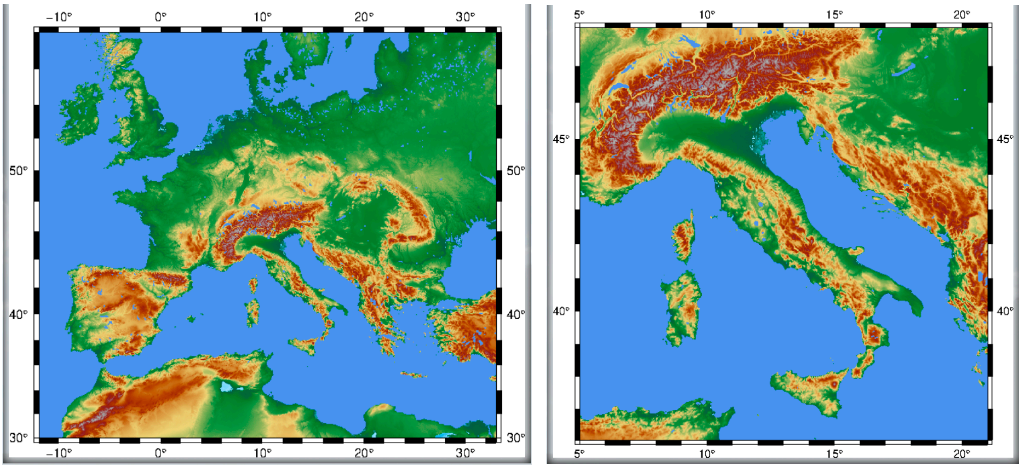

(**a**) (**b**)

Figure 1. CHIMBO integration domains: Europe (**a**) and Italy (**b**) with horizontal cell grids of ca. 20 km and ca. 8 km, respectively. The different colors indicate the orography: the sea surface is depicted in blue, brown shades for higher altitudes and green shades for lower altitudes or flat terrains are used.

The CHIMERE air quality model [22] has been widely used for studies on the urban scale to the regional scale, with typical horizontal grid resolution from 1 km for urban-scale domains to about 50 km for regional-scale domains. Several applications, from analysis of pollution events to forecast or long-term simulations, have been made and are available at the official CHIMERE web site (https://www.lmd.polytechnique.fr/chimere/CW-articles.php (accessed on 25 September 2024). The model includes processes of gas and aerosol chemistry, taking into account emissions, both anthropogenic and natural, and dry and wet deposition. Natural emissions, in addition to biogenic emissions, can include emissions of mineral dust, sea-salt aerosols and emissions from fires and volcanos. CHIMERE offers the option to include different gas phase chemical mechanisms, which are the complete MELCHIOR mechanism [36] adapted for low NOx conditions and NOx-nitrate chemistry, the reduced MELCHIOR mechanism [37] and the SAPRC-07-A mechanism [38]. It is also possible to include the dimethyl sulfide (DMS) chemistry, whose emissions contribute to SO_2 and sulfate. The aerosol chemistry and dynamics are included in CHIMERE using a size-bin approach, with the aerosol particles for each of the included species distributed in N size bins. The main aerosol processes considered are nucleation, coagulation and absorption. The particle/gas partitioning and the estimation of the gas-phase concentrations at equilibrium are computed using the thermodynamic equilibrium model. For the inorganic part containing ammonium, sulfates and nitrates, the model ISORROPIA [39] is used. The semi-volatile organic species are related to particle concentrations following the approach proposed [40]. Sulfur aqueous chemistry, a few heterogeneous reactions and the SOA formation from primary organic aerosols (POA) are taken into account. Details on the activated mechanism can be found in CHIMERE documentation freely available at the CHIMERE web page (https://www.lmd.polytechnique.fr/chimere/ (accessed on 25 September 2024)).

As stated above, since 2018, CNR-ISAC has made daily air quality forecasts over both European and Italian territories available. Such a modeling chain calculates the concentrations of major atmospheric components (gas and aerosols) using a nested configuration. The parent integration domain covers Europe (see Figure 1a) with ca. 20 km grid spacing, and the nested domain covers Italy (see Figure 1b), with horizontal resolutions of ca. 8 km. The vertical grid is based on eight atmospheric levels between 0 and 5700 m with different thicknesses, thinner near the ground. An automatic procedure is executed daily starting at 00:00 UTC, for generating a 72 h run in forecast mode.

The initial conditions of BOLAM are derived from the analyses (at 00:00 UTC of each day) of the GFS model (NOAA-NCEP). The boundary conditions are provided by the grid-point hydrostatic general circulation model GLOBO [41,42]. As for the sea surface temperature (SST), it is prepared by the CNR-ISMAR Institute in Rome using data provided from the Copernicus Marine Environment Monitoring Service (CMEMS).

On the other hand, initial and boundary conditions for atmospheric compounds are derived from the global circulation model for the atmospheric composition distributed by the European Centre of Medium-Range Weather Forecasts (ECMWF, https://www.ecmwf.int (accessed on 25 September 2024)) in the framework of the Copernicus Atmosphere Monitoring Service initiative (CAMS, https://atmosphere.copernicus.eu/ (accessed on 25 September 2024)), while the meteorological model BOLAM is driven by the Global Forecast System (GFS) made available by the National Oceanic and Atmospheric Administrational (NOAA) National Center for Environmental Prediction (NCEP) global analysis valid at 18:00 UTC. The anthropogenic emissions were provided by the TNO-MACC dataset [43], while the biogenic emissions were calculated by MEGAN v2.0 [44].

2.2. Meteorological Measurements

In the present, at ISAC-CNR, the main meteorological parameters simulated by BOLAM are verified using observed data. Model output is also compared with those of the NWP model IFS-ECMWF. Temperature at 2 m, dew point temperature at 2 m, wind speed at 10 m over surface, pressure at mean sea level, soil temperature and precipitation accumulated in 24 h at surface are compared with the SYNOP-Land data from WMO GTS, retrieved from the ECMWF archive. For all meteorological variables except soil moisture, for which there is less data availability, over the BOLAM domain, 2800 stations are available. In this work, we considered the ca. 100 SYNOP-Land stations located in Italian territory, as depicted in Figure 2.

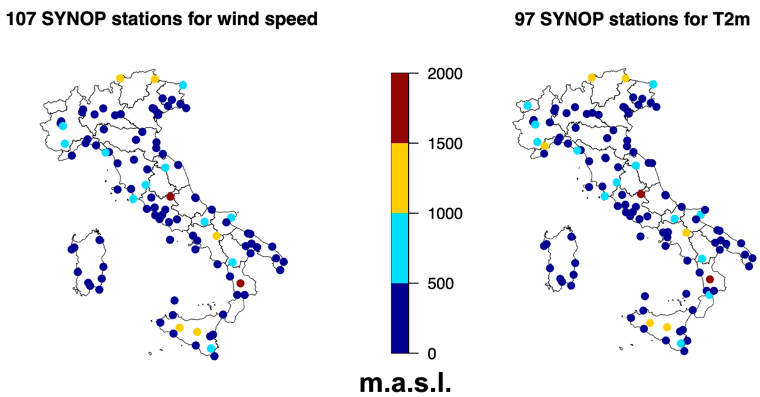

Figure 2. Locations of SYNOP-Land station for Italian peninsula where wind speed (**left panel**) and 2 m temperature (**right panel**) are measured and considered for this work. Color bar indicates the altitude of sampling sites.

For wind speed comparison, 107 sampling sites are considered, while for air temperature at 2 m, there are 97. The largest numbers of stations are located at altitudes less than 500 m (blue points in Figure 2); less than 10 sampling sites are at altitudes more than 1000 m above sea level. The sampling sites are almost homogeneously distributed on the national territory, and such a feature gives more robustness to the comparisons of such measurements with BOLAM model runs over an Italian integration domain with a grid spacing of ~8 km.

2.3. Ground-Based Concentration Observations over the Italian Domain

The measurement data utilized for model validation were sourced from the European Air Quality Portal (AQP), managed by the European Environmental Agency (EEA), encompassing the majority of European Member States. Specifically, primary validated assessment data—measurements (E1a dataset) flagged with the highest quality—were employed for comparison with model outputs. The analysis presented here exclusively considers monitoring stations with a minimum of 60% valid observations throughout the year. Assessments over the Italian territory were conducted using hourly data for O_3 and NO_2 and daily mean data for PM_{10} and $PM_{2.5}$. Table 1 outlines the number of background stations utilized for forecast evaluation by pollutant and classification.

Table 1. Type and number of background stations used for forecast evaluation per pollutant.

	Background		
	Urban	**Suburban**	**Rural**
O_3	133	81	60
NO_2	133	81	60
PM_{10}	104	42	37
$PM_{2.5}$	98	32	15

2.4. Air Quality Simulations: CAMS Ensemble Model

The CAMS ensemble model (https://atmosphere.copernicus.eu/cams-european-air-quality-ensemble-forecasts-welcomes-two-new-state-art-models (accessed on 25 September 2024)) is a state-of-the-art multi-model system that provides daily forecasts and analyses of atmospheric composition in Europe. It is part of the Copernicus Atmosphere Monitoring Service (CAMS), which is the European Union's flagship program for monitoring and understanding the Earth's atmosphere. It consists of eleven individual models that are developed and operated by different research institutes and meteorological services across Europe. Each model simulates the transport, chemistry, and deposition of various air pollutants, such as ozone, nitrogen dioxide, sulfur dioxide, particulate matter, and aerosols. The models use common emissions datasets and boundary conditions from the global CAMS system and are driven by high-resolution weather forecasts from the European Centre for Medium-Range Weather Forecasts (ECMWF) (https://atmosphere.copernicus.eu/regional-air-quality-production-systems (accessed on 25 September 2024)). The CAMS ensemble model combines the outputs of the individual models using a median-based approach, which gives more robust and reliable results than any single model. The ensemble also provides information on the uncertainty and variability of the forecasts, which is useful for decision making and risk assessment. The CAMS ensemble model covers a large domain that includes Iceland and the whole Mediterranean basin, with a spatial resolution of about 10 km $\times$ 10 km. The main products delivered are surface concentrations and vertical profiles of various pollutants. It is updated and improved regularly, with new models and features added to the system. The latest upgrade, which took place in June 2022, introduced two new models: MINNI, developed and operated by ENEA (Italy), and MONARCH, developed and operated by the Barcelona Supercomputing Centre (Spain). These models enhance the representation of aerosols and their interactions with clouds and radiation in the CAMS ensemble model. Such a model is a valuable tool for monitoring and forecasting air quality in Europe, as well as for assessing the impacts of air pollution on human health, ecosystems, and climate. The CAMS ensemble model data is freely available to the public and various users, such as environmental agencies, policymakers, researchers, media and citizens, through the CAMS website and the Atmosphere Data Store (ADS).

2.5. Measurements of Particulate Chemical Composition

A specific analysis on the ability of the model to simulate the chemical composition of particulate matter was conducted focusing on Northern Italy. Daily observations of PM_{10}

and/or $PM_{2.5}$ mass and PM_{10} or $PM_{2.5}$ chemical composition from the monitoring network of the regional Environmental Protection Agencies (ARPAs) of Emilia-Romagna, Lombardia and Valle D'Aosta have been used for the evaluation of the model to simulate different aerosol components, both primary and secondary. Table 2 shows the list of the aerosol species considered for the evaluation and of the stations for which the comparison between observations and simulations was possible throughout the year 2019 (even if with different temporal coverage for the different sites: some gaps or different protocols/schedules). The chemical composition of the Emilia-Romagna sites (i.e., Bologna, Parma, Rimini and San Pietro Capofiume) refers to $PM_{2.5}$, while all the others are relative to PM_{10}. The stations are representative of different types of sites: most of them (seven out of 11) are urban background sites, one of which, however (Aosta), is located at 545 m asl, in the middle of the Alps; two are instead urban traffic sites, and other two are considered rural background. Figure 3 shows the location of the sampling sites listed in Table 2.

Table 2. Sites and species for which daily measurements are used for comparison with model simulations. The chemical components when available were measured in PM_{10} for all the sites except for the ones marked by an asterisk (*) corresponding to the Emilia-Romagna ARPAE sites, where the chemical composition refers to $PM_{2.5}$. For each species at each site, the number of datapoints (i.e., number of days) covered by measurements is reported.

Site & Station Name	Site ID	Lat	Lon	Type	PM10	PM2.5	Sulfate	Nitrate	Ammonium	Chloride	EC	OC
Bologna Supersito	BO	44.52	11.34	Urban background	271	271	274 *	276 *	276 *	128 *	244 *	245 *
San Pietro Capofiume	SPC	44.65	11.62	Rural background	276	260	93 *	94 *	94 *	94 *	89 *	89 *
Parma	PR	44.79	10.33	Urban background	281	281	94 *	94 *	94 *	94 *	79 *	79 *
Rimini	RI	44.06	12.55	Urban background	272	272	97 *	97 *	97 *	97 *	81 *	81 *
Brescia–Villaggio Sereno	BS	45.51	10.19	Urban background	167	-	166	166	167	166	167	167
Lodi	LO	45.30	9.50	Urban background	46	-	46	46	46	46	46	46
Schivenoglia (MN)	Schi	45.02	11.08	Rural background	269	-	268	268	268	269	269	269
Milano-Pascal	MI_PA	45.48	9.23	Urban background	248	-	253	253	253	253	258	258
Milano-Marche	MI_MA	45.50	9.19	Urban traffic	259	-	144	144	138	144	143	143
Milano-Senato	MI_SE	45.47	9.20	Urban traffic	259	-	238	238	237	238	251	251
Aosta	AO	45.74	7.32	Urban background	-	-	288	288	288	288	113	113

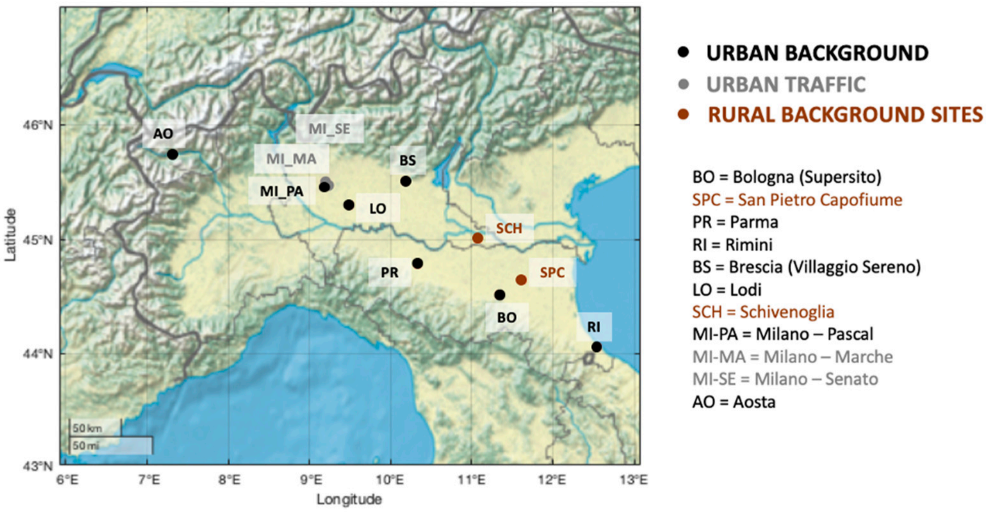

Figure 3. Location and names of the sites for which the observations vs. CHIMBO comparison was done throughout 2019.

3. Results

We performed an evaluation of the CHIMBO modeling chain performances over Italy for the year 2019. Model outputs were compared with (i) SYNOP meteorological observations, (ii) PM_{10}, $PM_{2.5}$, O_3 and NO_2 concentrations measurements made available by European Environmental Agency, (iii) CAMS ensemble model and (iv) the chemical composition measured at super sites located in Northern Italy.

3.1. Meteorological Parameters

We compared the time series of 2 m temperature and wind speed at 10 m predicted by the BOLAM meteorological model with SYNOP-Land measurement stations. These measures are representative of processes affecting the synoptic scale and are particularly suitable for comparing modeling simulations performed on the mesoscale domain. Figure 4 shows the time series of daily mean values comparisons of the above-mentioned meteorological variables for the period December 2018–February 2020.

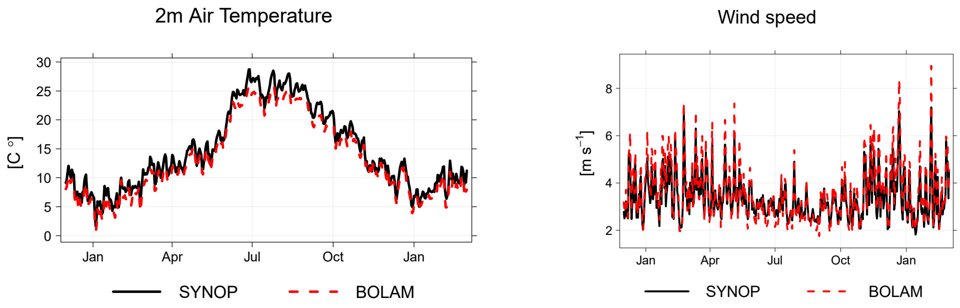

Figure 4. Time series of 2 m air temperature (**left panel**) and wind speed (**right panel**) of daily mean values as calculated over 97 and 107 SYNOP measurement stations (showed in Figure 2).

BOLAM captures the time variations throughout the seasons, even if a weak overall underestimation is pointed out over the considered period. On the other hand, the model tends to overestimate the wind speed during the cold seasons, especially in high wind speed conditions.

To evaluate the model performance, basic statistics are calculated and reported in Table 3. Pearson correlation R values are 0.99 and 0.97 for 2 m temperature and wind speed, respectively. The mean bias is negative for 2 m temperature and weakly positive for wind speed. The root mean square error is very close to zero for wind speed and 1.4 for 2 m temperature. These values indicate a high accuracy of the meteorological module; we can thus state that the meteorological variables we have shown are very well predicted by the BOLAM model. Nevertheless, a comprehensive model verification can be found at the official BOLAM model web page: https://www.isac.cnr.it/dinamica/projects/forecast_verif/ (accessed on 25 September 2024).

Table 3. Basic statistics calculated for 2 m temperature and wind speed.

	R	**MB**	**RMSE**
2 m temperature	0.998	−1.40	1.49
Wind speed	0.971	0.21	0.445

3.2. Concentration Data

The PM_{10}, $PM_{2.5}$, O_3 and NO_2 concentrations simulated by CHIMBO have been compared with those of EnsCAMS (CAMS ensemble models), considered as a benchmark in this work. In addition, model outputs have been compared with the available air quality measurements described in Section 2.2. The model verification has been done considering daily mean concentrations at ground level. Due to the model resolution, only rural background stations have been considered. Figure 5 shows the monthly mean values of PM_{10}, $PM_{2.5}$, O_3 and NO_2 concentrations at available stations (Airbase) compared with CHIMBO and EnsCAMS numerical results.

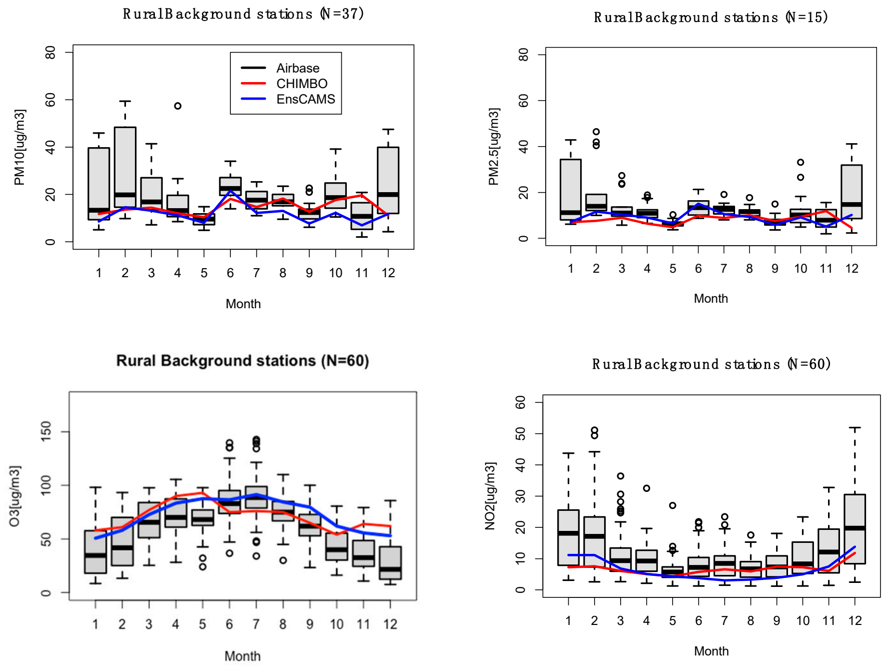

Figure 5. The comparisons of observed monthly median concentrations of PM_{10}, $PM_{2.5}$, O_3 and NO_2 (box plot (black and gray colors) with median, 25th and 75th percentiles and outliers), calculated by the CHIMBO modeling chain (red line) and the CAMS ensemble (blue line) are reported. The stations considered for this comparison are all those available nationwide for the year 2019 and representative of rural background conditions. In general, CHIMBO seems to have similar performances to the CAMS ensemble.

The median monthly values were calculated starting with daily values for the PM_{10} and $PM_{2.5}$ observations and with hourly ones for both O_3 and NO_2 measurements and numerical predictions. The annual average for PM_{10} levels is underestimated by both EnsCAMS and CHIMBO (Airbase: 19.6 μg m^{-3}, EnsCAMS: 14.1 μg m^{-3}, CHIMBO: 15.5 μg m^{-3}); $PM_{2.5}$ CHIMBO largely underestimates the annual mean with respect to measurements and EnsCAMS (Airbase: 13.9 μg m^{-3}, EnsCAMS: 11.2 μg m^{-3}, CHIMBO: 8.8 μg m^{-3}). On the other hand, for O_3, both EnsCAMS and CHIMBO overestimate the annual average (Airbase: 63 μg m^{-3}, EnsCAMS: 71 μg m^{-3}, CHIMBO: 70 μg m^{-3}), while for NO_2, as expected, the models predict lower concentrations than observed ones (Airbase: 11 μg m^{-3}, EnsCAMS: 8 μg m^{-3}, CHIMBO: 7 μg m^{-3}). Table 4 reports the mean bias (MB) and the root mean square error (RMSE) for CHIMBO and EnsCAMS calculated over a one-year period. We can state that while CHIMBO's predictions for NO_2 in summer and autumn are closer to the observed values, its overall annual trend is not well captured, as it calculates similar NO_2 concentrations across both cold and warm seasons. During the cold season, both EnsCAMS and CHIMBO tend to underestimate nitrogen dioxide (NO_2), while a significant overprediction of ozone (O_3) levels is pointed out. On the other hand, the annual behavior of O_3 and NO_2 appears quite different. CHIMBO cannot correctly reproduce the monthly ozone levels moving from spring to summer time, in which the season predicts an ozone concentration lower than the previous one. With regard to particulate matter, both CHIMBO and EnsCAMS underestimate concentration values during the cold season. The comparison between the two models shows that the largest discrepancies occur in the simulation of PM10, where CHIMBO demonstrates better performance, as reflected by the mean bias value. Nevertheless, the performance of CHIMBO and CAMS are comparable, at least for NO_2 and $PM_{2.5}$. However, further investigation is needed, principally in terms of emissions. As highlighted by the results presented in Section 3.3 concerning the chemical composition of PM_{10} and/or $PM_{2.5}$, NOx emissions could be underestimated, especially in rural areas. Another aspect to investigate involves the photochemical processes that dominate ozone and nitrogen dioxide formation and depletion.

Table 4. Mean bias and root mean square error calculated over one-year period for PM_{10}, $PM_{2.5}$, O_3 and NO_2 as predicted by CHIMBO and EnsCAMS.

	PM_{10}		$PM_{2.5}$		O_3		NO_2	
	MB	**RMSE**	**MB**	**RMSE**	**MB**	**RMSE**	**MB**	**RMSE**
CHIMBO	−1.5	4.5	−2.8	4.4	+14.2	24.7	−4.2	5.4
EnsCAMS	−4.0	4.6	−1.7	2.4	+15.2	17.2	−4.0	4.5

3.3. Evaluation Against Chemical Measurements in Northern Italy

The prediction skill metrics defined in Supplementary Material are used to evaluate CHIMBO outputs against daily ground measurements from the 11 stationary stations over Northern Italy, as summarized in Table 5 and Table S1. Chemical composition data were compared between available corresponding sizes (i.e., $PM_{2.5}$ for the Emilia-Romagna sites, BO, SPC, PR and RI and PM_{10} for all the others). The overall agreement between ground observations and model predictions is encouraging, as also shown by the scatter plots in Figure 6. The majority (71%) of the data points for total PM_{10} lie within the 1:2 and 2:1 error lines. The error is mostly scatter (FERROR = 0.49) rather than systematic bias (FBIAS = −0.29). CHIMBO predictions also agree reasonably well for the $PM_{10}/PM_{2.5}$ species. The measured annual average concentrations for nitrate, sulfate and ammonium were 4.91, 1.86 and 1.86 μgm^{-3}, respectively, compared to the predicted averages of 4.53, 1.08 and 1.65 μgm^{-3}. The comparison for particulate organic carbon (OC) and elemental carbon (EC) concentrations is similar to that for total PM_{10} mass (66% and 69% of the data are predicted within a factor of 2 for OC and EC, respectively, with FERROR = 0.57 and 0.54 and FBIAS = −0.31 and −0.04). In agreement with the ground measurements, the model predicts that organics and nitrate make up the largest portion of the $PM_{10}/PM_{2.5}$ total mass, followed by sulfate and ammonium. Nitrate is the worst predicted species at all the sites (overall only 49% of the data are predicted within a factor of 2 with FERROR = 0.80 and FBIAS = −0.31) but with a notable variation of model performance among the sites (Figure 6 and Table S1): in particular, the model underestimates nitrate concentrations in almost all the background sites (both rural and urban), while it tends to strongly overpredict NO3 in the urban traffic sites of Milano Senato (NMB = 32%). Among the different sites, the worst comparisons are obtained for Aosta, which, however, as already mentioned above, is a peculiar urban background site because it is located at >500 m asl, in a valley surrounded by mountains. This points out the difficulties of simulating pollutant concentrations at elevated/mountain sites, quite common to many CTMs. In fact, over mountains, a variety of airflows develop, such as dynamically driven [45], and/or thermally driven flows [45], requiring high horizontal resolutions (~1 km) to be better simulated [46]. In the case of Aosta, [47] has already suggested the occurrence of upwelling currents responsible for the transport of pollutants towards the valley from the Po basin, possibly responsible for the higher particulate matter concentrations observed in Aosta with respect to what CHIMBO reproduces.

The agreement between observations and model is also good for the urban traffic sites of Milan (i.e., Marche and Senato), and the agreement is even better for carbonaceous species (i.e., elemental and organic carbon, for which more than 75% of the data are predicted within a factor of 2). This at first glance seems to indicate that the model correctly estimates traffic emissions and well reproduces the concentrations of carbonaceous species in the sites dominated by such emissions.

Table 5. Prediction skill metrics of CHIMBO against daily ground measurements from all 11 stations in Northern Italy listed in Table 2 during 2019 taken all together.

	Mean Observed ($\mu g\ m^{-3}$)	Mean Predicted ($\mu g\ m^{-3}$)	NMB (%)	NME (%)	MB ($\mu g\ m^{-3}$)	MAGE ($\mu g\ m^{-3}$)	FBIAS	FERROR	Percent Within a Factor of 2
Overall									
PM_{10}	31.08	20.97	−28%	45%	−8.66	14.00	−0.29	0.49	71%
$PM_{2.5}$	18.44	13.44	−33%	64%	−6.03	11.81	−0.37	0.71	47%
Sulfate	1.86	1.08	−43%	58%	−0.81	1.08	−0.48	0.71	51%
Nitrate	4.91	4.53	−12%	55%	−0.58	2.72	−0.31	0.80	49%
Ammonium	1.86	1.65	−15%	53%	−0.27	0.99	0.00	0.64	58%
EC	0.99	0.78	−14%	54%	−0.14	0.53	−0.04	0.54	69%
OC	5.81	3.81	−29%	51%	−1.67	2.95	−0.31	0.57	66%

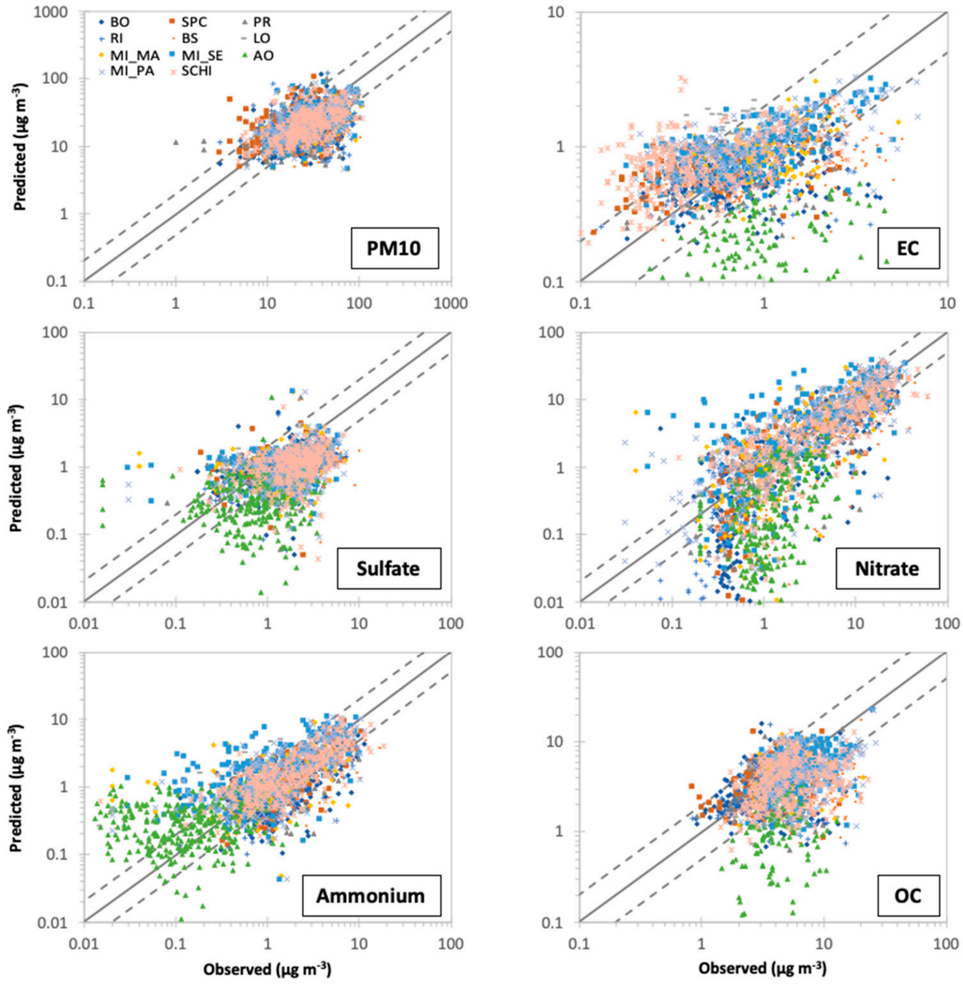

Figure 6. Comparison of predicted vs. observed PM_{10} mass and $PM_{10}/PM_{2.5}$ main chemical components concentrations ($\mu g m^{-3}$) from 11 measurement stations in Northern Italy during 2019. Each point corresponds to a 1-day average value. Also shown are the 1:1, 2:1 and 1:2 lines. Observed data represent gravimetric and chemical measurements. Carried out by ARPAs on filter samples.

In some background sites, however, even if on average the agreement between measured and simulated concentrations is good, there are some seasonal discrepancies. In Bologna, for example (as shown by the time series in Figure 7), we have an overestimation of OC during the summer and a strong underestimation during the winter. This can be the result of the possible overestimations in the emission/formation factors of biogenic OC during the summer and the underestimation (or total lack) of some sources of OC and EC during the winter. A possible explanation of this winter-time EC and OC underestimation can be related to the missing representation in the model of the ageing processes of biomass combustion emissions from domestic heating, recently suggested as an overlooked source of winter SOA by several experimental [25,27,48,49] and modeling studies [50–52].

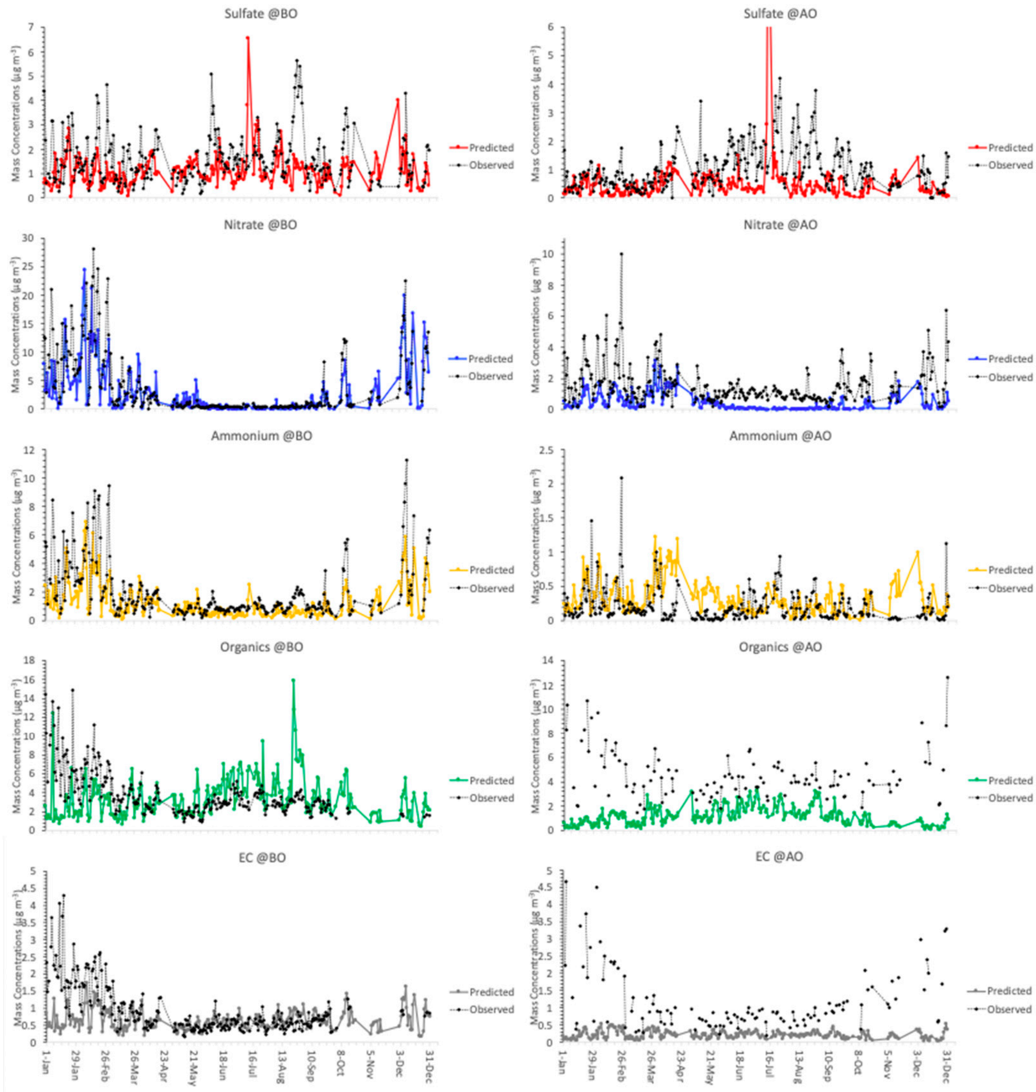

Figure 7. Time series of daily concentrations of different $PM_{10}/PM_{2.5}$ chemical components as measured and simulated by CHIMBO ("Observed" and "Predicted" in the legend, respectively) for the site of Bologna (BO) and Aosta (AO).

As for the summer overestimation, a revision of the biogenic emissions inventories and a better evaluation of their oxidation processes in the study area would be necessary to improve the simulations [53,54].

As shown in the time series in Figure 7, there is a general underestimation of all species at Aosta, except for ammonium, which is overestimated on average, as already mentioned. In particular, OC and EC are underestimated during winter. It appears that the EC simulated by the model remains constant among the seasons, while the observed one is much higher than predicted during winter. This could be imputed to the already discussed reasons (missing winter SOA formation) but also to misrepresentation of the transport from the polluted Po basin.

4. Conclusions

This paper reports the results of the CHIMBO modeling chain evaluation, carried out on the Italian domain and the Po Valley subdomain for a one-year-long period (i.e., 2019). In general, comparing simulated versus observed data, the CHIMBO performances are comparable with those reported in the literature for other state-of-the-art models. From the verification carried out on the whole Italian territory, it is clear that the CHIMBO chain is more suitable for studies aimed at quantitatively evaluating the distribution of pollutants on a regional scale, as in the case of the CAMS ensemble models. The analysis of the main chemical species of particulate matter shows that the CHIMBO model reproduces fairly well, on average, the concentrations of organic and elemental carbon and also of secondary inorganic compounds (sulfate, nitrate and ammonium), at least in the background stations in the plain terrain of Po Valley (i.e., all those considered except Aosta). Nevertheless, from the comparison of the time trends along the study year, clear seasonal discrepancies emerge in almost all the sites in specific periods and especially in winter when there are medium-to-strong underestimations of most of the species, especially EC and OC in the background sites. Such underestimations during the cold season are probably due to (i) underestimations of primary emissions (especially the combustion sources related to domestic heating), (ii) the low effectiveness of secondary formation processes in winter conditions (characterized by poor photochemistry and high relative humidity) and (iii) an excessive dilution of pollutants during calm wind conditions (overestimation of wind intensity).

In conclusion, the CHIMBO modeling chain—as a state-of-the-art modeling system—is considered an adequate numerical tool for a quantitative investigation of atmospheric composition over the mesoscale, even if some limitations remain due to the main issues related to the emissions inventories and the meteorology, which are the major atmospheric processes drivers.

Supplementary Materials: The following supporting information can be downloaded at https://www.mdpi.com/article/10.3390/atmos15111386/s1: Table S1: Prediction skill metrics of CHIMBO against daily ground measurements from every single station of the 11 sites in Northern Italy listed in Table 2 during 2019.

Author Contributions: The initial conception and the paper structure were done by T.C.L. and M.P., T.C.L. and O.D. executed all model runs. T.C.L. and M.M. elaborated the AIRBASE and SYNOP datasets for the comparisons over the Italian domain. M.P. dealt with the elaborations and the comparisons of chemical atmospheric compounds over Northern Italy. T.C.L., M.P., R.C., O.D. and M.M. discussed the model results. F.R. and F.M.G. provided the technical support for numerical simulations over the HPC infrastructure. R.C. provided her support in writing and reviewing the paper during its preparation. T.C.L., M.P. and R.C. wrote the final version of the paper. All authors have read and agreed to the published version of the manuscript.

Funding: National Recovery and Resilience Plan (NRRP), Mission 04 Component 2 Investment 1.5—NextGenerationEU, call for tender n. 3277 dated 30/12/2021. Award Number: 0001052 dated 23 June 2022 (ECS_00000033_ECOSISTER).

Institutional Review Board Statement: Not applicable.

Informed Consent Statement: Not applicable.

Data Availability Statement: The raw data supporting the conclusions of this article will be made available by the authors on request from the list reported in the "Instructions for Authors" web page (https://www.mdpi.com/journal/atmosphere/instructions#suppmaterials, accessed on 18 July 2024). There are not ethical or privacy reasons, the data are just available to everybody on request.

Acknowledgments: This study was supported by the National Recovery and Resilience Plan (NRRP), Mission 04 Component 2 Investment 1.5—NextGenerationEU, call for tender n. 3277 dated 30/12/2021. Award Number: 0001052 dated 23/06/2022 (ECS_00000033_ECOSISTER). The authors gratefully thank the personnel of the Regional Environmental Protection Agencies (ARPAs) of Emilia-Romagna (D. Bacco, A. Trentini and V. Poluzzi of the Centro Tematico Regionale Qualità dell'Aria at Bologna), Lombardia (Cristina Colombi of the UO Qualità dell'Aria in Milan) and Valle d'Aosta (M. Zublena, T. Magri, I. Tombolato, and H. Diémoz of the Sezione Aria, atmosfera e pressioni sull'ambiente at Aosta).

Conflicts of Interest: The authors declare no conflicts of interest.

References

1. de Vries, W.; Posch, M.; Simpson, D.; de Leeuw, F.A.A.M.; van Grinsven, H.J.M.; Schulte-Uebbing, L.F.; Sutton, M.A.; Ros, G.H. Trends and Geographic Variation in Adverse Impacts of Nitrogen Use in Europe on Human Health, Climate, and Ecosystems: A Review. *Earth-Sci. Rev.* **2024**, *253*, 104789. [CrossRef]
2. Mitchell, J.F.B. The "Greenhouse" Effect and Climate Change. *Rev. Geophys.* **1989**, *27*, 115–139. [CrossRef]
3. Vitousek, P.M.; Mooney, H.A.; Lubchenco, J.; Melillo, J.M. Human Domination of Earth's Ecosystems. *Science* **1997**, *277*, 494–499. [CrossRef]
4. WHO Global Air QUALITY guidelines. In *Particulate Matter (PM2.5 and PM10), Ozone, Nitrogen Dioxide, Sulfur Dioxide and Carbon Monoxide*; World Health Organization: Geneva, Switzerland, 2021. Available online: https://iris.who.int/handle/10665/345329 (accessed on 25 September 2024).
5. Wang, F.; Harindintwali, J.D.; Yuan, Z.; Wang, M.; Wang, F.; Li, S.; Yin, Z.; Huang, L.; Fu, Y.; Li, L.; et al. Technologies and Perspectives for Achieving Carbon Neutrality. *Innovation* **2021**, *2*, 100180. [CrossRef]
6. Chu, H.; Huang, Z.; Zhang, Z.; Yan, X.; Qiu, B.; Xu, N. Integration of Carbon Emission Reduction Policies and Technologies: Research Progress on Carbon Capture, Utilization, and Storage Technologies. *Sep. Purif. Technol.* **2024**, *343*, 127153. [CrossRef]
7. IPCC. 2022: Summary for Policymakers. In *Climate Change 2022: Impacts, Adaptation and Vulnerability. Contribution of Working Group II to the Sixth Assessment Report of the Intergovernmental Panel on Climate Change*; Pörtner, H.-O., Roberts, D.C., Tignor, M., Poloczanska, E.S., Mintenbeck, K., Alegría, A., Craig, M., Langsdorf, S., Löschke, S., Möller, V., et al., Eds.; Cambridge University Press: Cambridge, UK; New York, NY, USA, 2023; pp. 3–33. [CrossRef]
8. Bonazza, A.; Messina, P.; Sabbioni, C.; Grossi, C.M.; Brimblecombe, P. Mapping the impact of climate change on surface recession of carbonate buildings in Europe. *Sci. Total Environ.* **2009**, *407*, 2039–2050. [CrossRef] [PubMed]
9. Spezzano, P. Mapping the susceptibility of UNESCO World Cultural Heritage sites in Europe to ambient (outdoor) air pollution. *Sci. Total Environ.* **2021**, *754*, 142345. [CrossRef]
10. Bonazza, A.; Sardella, A. Climate change and cultural heritage: Methods and approaches for damage and risk assessment addressed to a practical application. *Heritage* **2023**, *6*, 3578–3589. [CrossRef]
11. Dechezleprêtre, A.; Koźluk, T.; Kruse, T.; Nachtigall, D.; De Serres, A. Do Environmental and Economic Performance Go Together? A Review of Micro-Level Empirical Evidence from the Past Decade or So. *Int. Rev. Environ. Resour. Econ.* **2019**, *13*, 1–118. [CrossRef]
12. EEA: Europe's Air Quality Status 2024, EEA Briefing no. 06/2024. Available online: https://www.eea.europa.eu//publications/europes-air-quality-status-2024 (accessed on 6 November 2024).
13. Zhang, Y.; Bocquet, M.; Mallet, V.; Seigneur, C.; Baklanov, A. Real-time air quality forecasting, part I: History, techniques, and current status. *Atmos. Environ.* **2012**, *60*, 632–655. [CrossRef]
14. Zhang, Y.; Bocquet, M.; Mallet, V.; Seigneur, C.; Baklanov, A. Real-time air quality forecasting, Part II: State of the science, current research needs, and future prospects. *Atmos. Environ.* **2012**, *60*, 656–676. [CrossRef]
15. Mailler, S.; Menut, L.; Khvorostyanov, D.; Valari, M.; Couvidat, F.; Siour, G.; Turquety, S.; Briant, R.; Tuccella, P.; Bessagnet, B.; et al. CHIMERE-2017: From urban to hemispheric chemistry-transport modeling. *Geosci. Model Dev.* **2017**, *10*, 2397–2423. [CrossRef]
16. Simpson, D.; Benedictow, A.; Berge, H.; Bergström, R.; Emberson, L.D.; Fagerli, H.; Flechard, C.R.; Hayman, G.D.; Gauss, M.; Jonson, J.E.; et al. The EMEP MSC-W chemical transport model—Technical description. *Atmos. Chem. Phys.* **2012**, *12*, 7825–7865. [CrossRef]
17. Grell, G.A.; Peckham, S.E.; Schmitz, R.; McKeen, S.A.; Frost, G.; Skamarock, W.C.; Eder, B. Fully coupled 'online' chemistry in the WRF model. *Atmos. Environ.* **2005**, *39*, 6957–6976. [CrossRef]
18. Monks, P.S.; Granier, C.; Fuzzi, S.; Stohl, A.; Williams, M.L.; Akimoto, H.; Amann, M.; Baklanov, A.; Baltensperger, U.; Bey, I.; et al. Atmospheric Composition Change—Global and Regional Air Quality. *Atmos. Environ.* **2009**, *43*, 5268–5350. [CrossRef]
19. Peuch, V.-H.; Engelen, R.; Rixen, M.; Dee, D.; Flemming, J.; Buontempo, C. The Copernicus Atmosphere Monitoring Service from Research to Operations. *Bull. Am. Meteorol. Soc.* **2022**, *103*, E2650–E2668. [CrossRef]
20. Marécal, V.; Peuch, V.-H.; Andersson, C.; Andersson, S.; Arteta, J.; Beekmann, M.; Benedictow, A.; Bergström, R.; Bessagnet, B.; Cansado, A.; et al. A regional air quality forecasting system over Europe: The MACC-II daily ensemble production. *Geosci. Model Dev.* **2015**, *8*, 2777–2813. [CrossRef]
21. Davolio, S.; Buzzi, A.; Malguzzi, P. Orographic triggering of long-lived convection in three dimensions. *Meteorol. Atmos. Phys.* **2009**, *103*, 35–44. [CrossRef]
22. Menut, L.; Bessagnet, B.; Khvorostyanov, D.; Beekmann, M.; Blond, N.; Colette, A.; Coll, I.; Curci, G.; Foret, G.; Hodzic, A.; et al. CHIMERE 2013: A model for regional atmospheric composition modelling. *Geosci. Model Dev.* **2013**, *6*, 981–1028. [CrossRef]
23. Cesari, R.; Landi, T.C.; D'Isidoro, M.; Mircea, M.; Russo, F.; Malguzzi, P.; Tampieri, F.; Maurizi, A. The On-Line Integrated Mesoscale Chemistry Model BOLCHEM. *Atmosphere* **2021**, *12*, 192. [CrossRef]

24. Ricciardelli, I.; Bacco, D.; Rinaldi, M.; Bonafè, G.; Scotto, F.; Trentini, A.; Bertacci, G.; Ugolini, P.; Zigola, C.; Rovere, F.; et al. A three-year investigation of daily PM2.5 main chemical components in four sites: The routine measurement program of the Supersito Project (Po Valley, Italy). *Atmos. Environ.* **2017**, *152*, 418–430. [CrossRef]
25. Gilardoni, S.; Massoli, P.; Paglione, M.; Giulianelli, L.; Carbone, C.; Rinaldi, M.; Decesari, S.; Sandrini, S.; Costabile, F.; Gobbi, G.P.; et al. Direct observation of aqueous secondary organic aerosol from biomass burning emissions. *Proc. Natl. Acad. Sci. USA* **2016**, *113*, 10013–10018. [CrossRef] [PubMed]
26. Decesari, S.; Sowlat, M.H.; Hasheminassab, S.; Sandrini, S.; Gilardoni, S.; Facchini, M.C.; Fuzzi, S.; Sioutas, C. Enhanced toxicity of aerosol in fog conditions in the Po Valley, Italy. *Atmos. Chem. Phys.* **2017**, *17*, 7721–7773. [CrossRef]
27. Paglione, M.; Gilardoni, S.; Rinaldi, M.; Decesari, S.; Zanca, N.; Sandrini, S.; Giulianelli, L.; Bacco, D.; Ferrari, S.; Poluzzi, V.; et al. The Impact of Biomass Burning and Aqueous-Phase Processing on Air Quality: A Multi-Year Source Apportionment Study in the Po Valley, Italy. *Atmos. Chem. Phys.* **2020**, *20*, 1233–1254. [CrossRef]
28. Pernigotti, D.; Georgieva, E.; Thunis, P.; Bessagnet, B. Impact of Meteorological Modelling on Air Quality: Summer and Winter Episodes in the Po Valley (Northern Italy). *Int. J. Environ. Pollut.* **2012**, *50*, 111–119. [CrossRef]
29. Pernigotti, D.; Georgieva, E.; Thunis, P.; Bessagnet, B. Impact of Meteorology on Air Quality Modeling over the Po Valley in Northern Italy. *Atmos. Environ.* **2012**, *51*, 303–310. [CrossRef]
30. Pernigotti, D.; Thunis, P.; Cuvelier, C.; Georgieva, E.; Gsella, A.; De Meij, A.; Pirovano, G.; Balzarini, A.; Riva, G.M.; Carnevale, C.; et al. POMI: A Model Intercomparison Exercise over the Po Valley. *Air Qual. Atmos. Health* **2013**, *6*, 701–715. [CrossRef]
31. Cesari, R.; Landi, T.; Maurizi, A. The coupled chemistry-meteorology model BOLCHEM: An application to air pollution in the Po Valley (Italy) hot spot. *Int. J. Environ. Pollut.* **2019**, *65*, 1–24. [CrossRef]
32. Veratti, G.; Stortini, M.; Amorati, R.; Bressan, L.; Giovannini, G.; Bande, S.; Bissardella, F.; Ghigo, S.; Angelino, E.; Colombo, L.; et al. Impact of NO_x and NH_3 Emission Reduction on Particulate Matter across Po Valley: A LIFE-IP-PREPAIR Study. *Atmosphere* **2023**, *14*, 762. [CrossRef]
33. Buzzi, A.; Fantini, M.; Malguzzi, P.; Nerozzi, F. Validation of a limited area model in cases of Mediterranean cyclogenesis: Surface fields and precipitation scores. *Meteorol. Atmos. Phys.* **1994**, *53*, 137–153. [CrossRef]
34. Nagata, M.; Leslie, L.; Kamahori, H.; Nomura, R.; Mino, H.; Kurihara, Y.; Rogers, E.; Elsberry, R.L.; Basu, B.K.; Buzzi, A.; et al. A mesoscale model intercomparison: A case of explosive development of a tropical cyclone (COMPARE III). *J. Meteorol. Soc. Jpn.* **2001**, *79*, 999–1033. [CrossRef]
35. Lagouvardos, K.; Kotroni, V.; Koussis, A.; Feidas, C.; Buzzi, A.; Malguzzi, P. The meteorological model BOLAM at the National Observatory of Athens: Assessment of two-year operational use. *J. Appl. Meteor.* **2003**, *42*, 1667–1678. [CrossRef]
36. Lattuati, M. Contribution a' L'e´tude du Bilan de L'ozone Troposphe´ Rique a' L'interface de L'europe et de l'Atlantique Nord: Mode´Lisation Lagrangienne et Mesures en Altitude. Ph.D. Thesis, University Pierre et Marie Curie, Paris, France, 1997.
37. Derognat, C.; Beekmann, M.; Baeumle, M.; Martin, D.; Schmidt, H. Effect of Biogenic Volatile Organic Compound Emissions on Tropospheric Chemistry During the Atmospheric Pollution over the Paris Area (ESQUIF) Campaign in the Ile-de-France Region. *J. Geophys. Res.* **2003**, *108*, 8560. [CrossRef]
38. Carter William, P.L. Development of the SAPRC-07 chemical mechanism. *Atmos. Environ.* **2010**, *44*, 5324–5335. [CrossRef]
39. Nenes, A.; Pandis, S.N.; Pilinis, C. ISORROPIA: A new thermodynamic equilibrium model for multiphase multicomponent inorganic aerosols. *Aquat. Geochem.* **1998**, *4*, 123–152. [CrossRef]
40. Pankow, J.F. An absorption model of the gas/aerosol partitioning involved in the formation of secondary organic aerosol. *Atmos. Environ.* **2007**, *41*, S75–S79. [CrossRef]
41. Malguzzi, P.; Buzzi, A.; Drofa, O. The Meteorological Global Model GLOBO at the ISAC-CNR of Italy: Assessment of 1.5 Yr of Experimental Use for Medium-Range Weather Forecast. *Weather Forecast.* **2011**, *26*, 1045–1055. [CrossRef]
42. Mastrangelo, D.; Malguzzi, P.; Rendina, C.; Drofa, O.; Buzzi, A. First Outcomes from the CNR-ISAC Monthly Forecasting System. *Adv. Sci. Res.* **2012**, *8*, 77–82. [CrossRef]
43. Kuenen, J.; Visschedijk, A.; Jozwicka, M.; Denier Van Der Gon, H. TNO-MACC_II emission inventory; a multi-year (2003–2009) consistent high-resolution European emission inventory for air quality modelling. *Atmos. Chem. Phys.* **2014**, *14*, 10963–10976. [CrossRef]
44. Guenther, A.; Karl, T.; Harley, P.; Wiedinmyer, C.; Palmer, P.I.; Geron, C. Estimates of Global Terrestrial Isoprene Emissions Using MEGAN (Model of Emissions of Gases and Aerosols from Nature). *Atmos. Chem. Phys.* **2006**, *6*, 3181–3210. [CrossRef]
45. Jackson, P.L.; Mayr, G.; Vosper, D. *Dynamically-Driven Winds. In Mountain Weather Research and Forecasting*; Chow, F.K., De Wekker, D.F.J., Snyder, B.J., Eds.; Springer: Dordrecht, The Netherlands, 2013; pp. 35–119, 121–218. [CrossRef]
46. Schmidli, J.; Böing, S.; Fuhrer, O. Accuracy of Simulated Diurnal Valley Winds in the Swiss Alps: Influence of Grid Resolution, Topography Filtering, and Land Surface Datasets. *Atmosphere* **2018**, *9*, 196. [CrossRef]
47. Diémoz, H.; Barnaba, F.; Magri, T.; Pession, G.; Dionisi, D.; Pittavino, S.; Tombolato, I.K.F.; Campanelli, M.; Della Ceca, L.S.; Hervo, M.; et al. Transport of Po Valley Aerosol Pollution to the Northwestern Alps—Part 1: Phenomenology. *Atmos. Chem. Phys.* **2019**, *19*, 3065–3095. [CrossRef]
48. Kodros, J.K.; Papanastasiou, D.K.; Paglione, M.; Masiol, M.; Squizzato, S.; Florou, K.; Skyllakou, K.; Kaltsonoudis, C.; Nenes, A.; Pandis, S.N. Rapid Dark Aging of Biomass Burning as an Overlooked Source of Oxidized Organic Aerosol. *Proc. Natl. Acad. Sci. USA* **2020**, *117*, 33028–33033. [CrossRef]

49. Florou, K.; Kodros, J.K.; Paglione, M.; Jorga, S.; Squizzato, S.; Masiol, M.; Uruci, P.; Nenes, A.; Pandis, S.N. Characterization and Dark Oxidation of the Emissions of a Pellet Stove. *Environ. Sci. Atmos.* **2023**, *3*, 1319–1334. [CrossRef]
50. Tsimpidi, A.P.; Karydis, V.A.; Pandis, S.N.; Lelieveld, J. Global combustion sources of organic aerosols: Model comparison with 84 AMS factor-analysis data sets. *Atmos. Chem. Phys.* **2016**, *16*, 8939–8962. [CrossRef]
51. Meroni, A.; Pirovano, G.; Gilardoni, S.; Lonati, G.; Colombi, C.; Gianelle, V.; Paglione, M.; Poluzzi, V.; Riva, G.; Toppetti, A. Investigating the role of chemical and physical processes on organic aerosol modelling with CAMx in the Po Valley during a winter episode. *Atmos. Environ.* **2017**, *171*, 126–142. [CrossRef]
52. Li, J.; Zhang, H.; Li, L.; Ye, F.; Wang, H.; Guo, S.; Zhang, N.; Qin, M.; Hu, J. Modeling secondary organic aerosols in China: State of the art and perspectives. *Curr. Pollut. Rep.* **2023**, *9*, 22–45. [CrossRef]
53. Jiang, J.; Aksoyoglu, S.; El-Haddad, I.; Ciarelli, G.; Denier van der Gon, H.A.C.D.; Canonaco, F.; Gilardoni, S.; Paglione, M.; Minguillón, M.C.; Favez, O.; et al. Sources of organic aerosols in Europe: A modeling study using CAMx with modified volatility basis set scheme. *Atmos. Chem. Phys.* **2019**, *19*, 15247–15270. [CrossRef]
54. Basla, B.; Agresti, V.; Balzarini, A.; Giani, P.; Pirovano, G.; Gilardoni, S.; Paglione, M.; Colombi, C.; Belis, C.A.; Poluzzi, V.; et al. Simulations of Organic Aerosol with CAMx over the Po Valley during the Summer Season. *Atmosphere* **2022**, *13*, 1996. [CrossRef]